Available online at www.sciencedirect.com

SCIENCE DIRECT

Virology 336 (2005) 100–112

VIROLOGY

www.elsevier.com/locate/yviro

Encapsidation of minute virus of mice DNA: Aspects of the translocation mechanism revealed by the structure of partially packaged genomes

Susan F. Cotmore[a], Peter Tattersall[a,b,*]

[a]*Department of Laboratory Medicine, Yale University Medical School, 333 Cedar Street, New Haven, CT 067510, USA*
[b]*Department of Genetics, Yale University Medical School, 333 Cedar Street, New Haven, CT 067510, USA*

Received 2 January 2005; returned to author for revision 22 February 2005; accepted 8 March 2005
Available online 12 April 2005

Abstract

Minute virus of mice (MVM) packages a single, negative-sense copy of its linear single-stranded DNA genome, but a chimeric virus, MML, in which >95% MVM sequence was fused to the right-hand terminus of LuIII, packages >40% positive-sense DNA. While encapsidation of both MML strands begins efficiently, genome translocation frequently stalls at specific sites in positive-sense DNA. Internalized sequences, derived from the 3′ end of the strand, ranged from 1 to 5 kb in length, with species of around 2 kb predominating. When nuclease activity during isolation was minimized, these truncated species were found to be part of pre-excised 5 kb single-strands. Similarly, some partially encapsidated negative-sense DNAs were observed, forming a continuum of protected 3′ sequences between 1 and 3 kb in length, but these were less abundant and more uniformly distributed than their positive-sense counterparts, indicating that the negative strand has evolved for efficient internalization. The paucity of protected DNAs shorter than 1–2 kb suggests that translocation is biphasic, proceeding efficiently through the first (3′) third of the genome, but prone to stall thereafter. Sequences with conspicuous secondary structure, including stem–loop and guanidine rich regions, were found to interrupt packaging, especially when positioned near the 5′ end of the strand. Since VP2 amino-terminal peptides were exposed at the particle surface in all packaging intermediates, extrusion of this peptide precedes translocation of the full-length strand.

Keywords: *Parvovirus*; MVM; LuIII; Packaging; 3′ - to-5′ encapsidation; Virion assembly; 3′ - to-5′ helicase; Packaging motor; DNA secondary structure

Introduction

Members of the family *Parvoviridae* package a single copy of their ~5 kb, single-stranded, linear DNA genome into a pre-formed, non-enveloped, protein capsid (King et al., 2001; Myers and Carter, 1980; Richards et al., 1977; Yuan and Parrish, 2001), but these viruses are unusual in that they can encapsidate strands of one or both polarities. Notably, while some family members, such as the adeno-associated viruses (AAVs), package both strand senses with equal frequency, members of the genus *Parvovirus* package either predominantly negative-sense DNA or strands of both polarities (Tattersall et al., 2005). Viral replication proceeds through a series of duplex intermediates, via a unidirectional strand-displacement mechanism called rolling-hairpin replication (Cotmore and Tattersall, 1995), driven from replication origins positioned at each end of the linear genome. We have recently shown that the polarity of strands selected for encapsidation is determined by the relative efficiency of these two telomeric origins, rather than by sense-specific packaging signals. This is apparently because relative origin efficiency ultimately determines the proportion of single-stranded negative and positive-sense DNAs that are displaced from duplex replication intermediates during the packaging phase of viral DNA amplification. All such displaced strands then appear to remain associated with the replicating DNA (Cotmore and Tattersall, 2005), perhaps through protein mediated interactions, and to serve as

* Corresponding author. Department of Laboratory Medicine, Yale University Medical School, 333 Cedar Street, New Haven, CT 067510, USA. Fax: +1 203 688 7340.
E-mail address: peter.tattersall@yale.edu (P. Tattersall).

0042-6822/$ - see front matter © 2005 Elsevier Inc. All rights reserved.
doi:10.1016/j.virol.2005.03.007

equivalent candidates for encapsidation, as suggested by the kinetic hairpin model previously proposed by Chen et al. (1989). This explains why parvoviruses with ITRs always generate and package equal numbers of plus and minus strands, while viruses with different sequences at each end mostly do not. In consequence, while Minute Virus of Mice (MVM) normally packages predominantly negative-sense strands, by switching its right-end origin with a similar, but less efficient, sequence from the closely-related virus LuIII, we were able to generate a chimeric virus, MML, that comprises the entire MVM coding sequence but packages more than 40% positive-sense DNA (Cotmore and Tattersall, 2005).

Parvoviruses encode a large replication initiator protein, called NS1 in MVM and Rep68/78 in the AAVs. This non-structural polypeptide comprises two distinct enzymatic domains: a region in the amino-terminal half of the molecule that exhibits site-specific duplex DNA binding activity and contains the enzymatic core of a site-specific single-strand nuclease (Hickman et al., 2004; Koonin and Ilyina, 1993; Nuesch et al., 1995); and, in its carboxy-terminal half, a superfamily III, 3′ - to-5′ helicase domain, which belongs to a group of viral enzymes evolutionarily related to the extensive AAA+ family of cellular ATPases (Christensen and Tattersall, 2002; Gorbalenya et al., 1990; Iyer et al., 2004; James et al., 2003). In the AAVs, this second domain can be accessed independently, from an additional viral promoter at map unit 19 (P19), giving rise to the small Rep polypeptides, Rep40/52, which are known to be essential for the efficient production of progeny virus (Chejanovsky and Carter, 1989). King et al. (2001) showed that this requirement depended upon the helicase activity of Rep40/52, and acted at the level of DNA translocation into the particle. As part of their role in melting duplex DNA, such helicases scan in a 3′ - to-5′ direction along a single DNA strand, driven by energy derived from ATP hydrolysis. DNase protection studies suggested that insertion of progeny strands into AAV particles proceeds from the 3′ end, which correlates with the 3′ - to-5′ processivity of the helicase. This observation led King et al. (2001) to suggest that Rep 40/52 molecules function as a molecular motor that becomes immobilized at a single capsid portal and effectively pumps the DNA into its virion. In their studies, it was apparent that this role could also be fulfilled, albeit much less efficiently, by the large Rep 68 and Rep 78 molecules. However, in this case, the extreme 5′ ends of the genomes were rarely internalized, suggesting that the small Reps are uniquely adapted to mediate complete strand translocation. To date, no functionally equivalent polypeptides, which do not bind site-specifically to duplex viral DNA but possess helicase activity and mediate strand translocation, have been identified for MVM.

Much less is known about the packaging mechanism in MVM. Virions containing specific types of defective subgenomic DNAs have been described, derived from high multiplicity infections with wild type virus (Faust and Ward, 1979). Although these defective particles were the result of aberrant replication, rather than incomplete packaging, analysis of their structures did much to further our understanding of the cis-acting sequences responsible for both viral replication and encapsidation. These deleted forms varied in size, from 0.5 to 3 kb, and fell into two distinct types: type I defectives, which carried internal deletions within the coding region of the virus but had both palindromic viral telomeres intact; and type II defectives, derived exclusively from the right-end of the genome (map units 85–100), which were double-stranded hairpin molecules whose complementary strands were covalently continuous. While individual defective genomes each contained two telomeres, albeit both from the right-hand end of the genome in type II defectives, they often had little other sequence in common, suggesting that at least the right-end terminus was essential for packaging.

In the present study, we have analyzed the stalled translocation products generated by the chimeric derivative, MML, in which >95% of the MVM sequence is fused to the right-hand terminus of LuIII. This virus attempts to encapsidate both positive- and negative-sense genomic sequences, but encounters difficulty in internalizing specific elements in the plus strand. As a result, successfully packaged full-length positive-sense MML DNAs were found to be rare, whereas partially packaged genomes accumulated to high levels in infected cells. This suggests that the negative-strand sequence of MVM has been under selective pressure to optimize its compatibility with the encapsidation mechanism, whereas the positive-strand sequence has not. Accumulation of these stalled complexes allowed us to explore the structure of the packaging intermediates and to determine what types of DNA sequences impede strand translocation.

Results

MML packages approximately equal numbers of each genomic strand, but positive strand packaging is mostly incomplete

The chimeric virus MML, derived predominantly (95.2%) from the prototype strain of MVM (MVMp), has been described previously (Cotmore and Tattersall, 2005), and contains the LuIII right-end hairpin (4.8%), as illustrated in Fig. 1A, which has a relatively inefficient replication origin. As a result, displacement of negative-sense DNA strands from the right-end of the genome, which normally predominates during the packaging phase of MVM DNA amplification, is impaired. This appears to cause the MML replication pathway to be diverted through a series of dimeric intermediates that support displacement and packaging of positive-sense DNA, causing virion populations of MML to contain both negative and positive-sense single strands (Cotmore and Tattersall, 2005). In

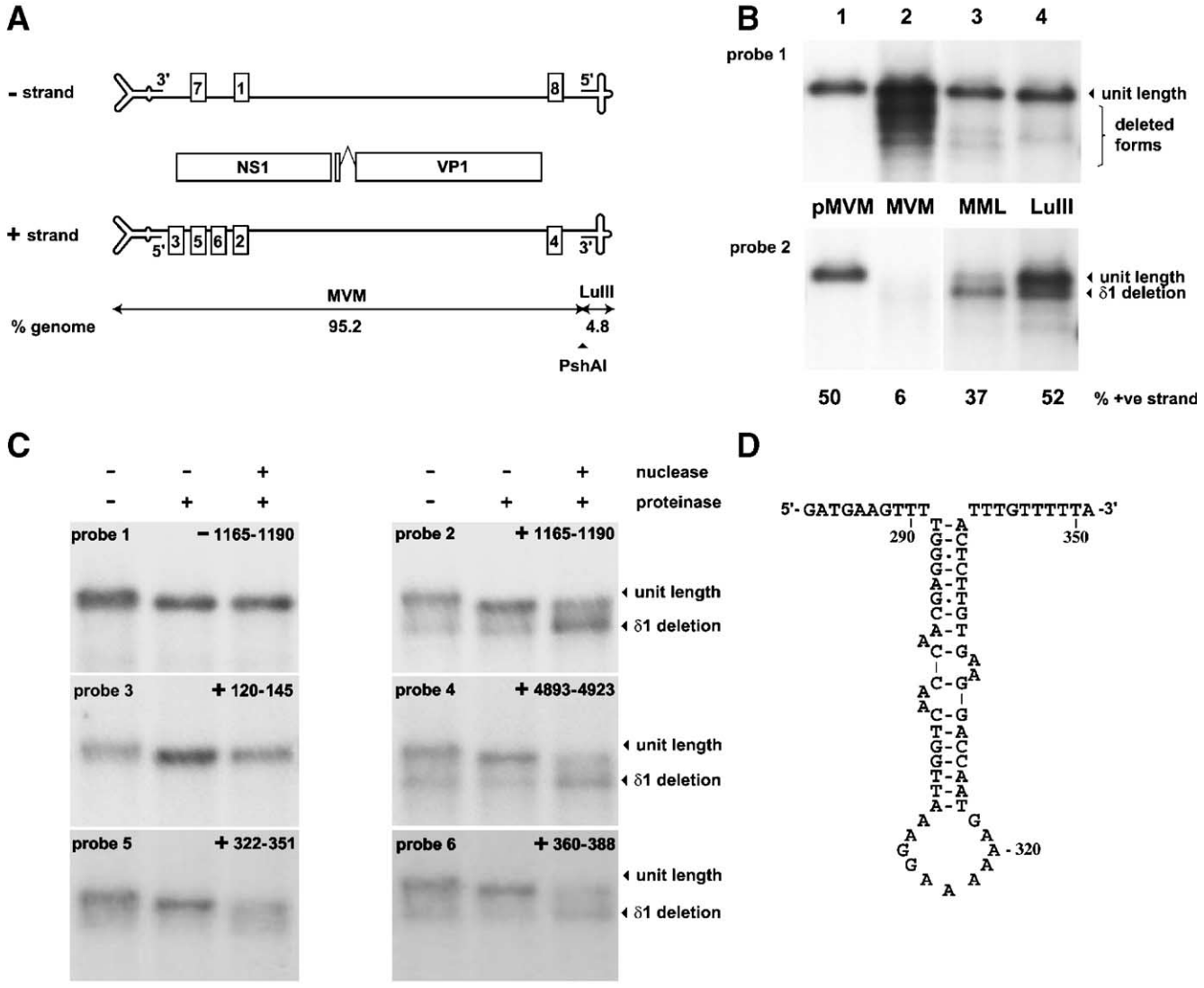

Fig. 1. MML packages both strands with different efficiencies. Panel A: diagram of the positive and negative strands of the MML genome showing, in numbered blocks, the sequences recognized by oligonucleotide probes 1 through 8. Probes 1 and 2 hybridize to the sequence between nucleotides 1165 and 1190 on the minus and plus strands, respectively; probe 3 hybridizes to nucleotides 120–145, probe 4 binds nucleotides 4893–4923, probe 5 binds nucleotides 322–351, and probe 6 binds nucleotides 360–388, all on the plus strand; probe 7 hybridizes to nucleotides 207–233, and probe 8 binds nucleotides 4850–4874, both on the minus strand. Nucleotide numbers are from GenBank accession number J02275, and follow the positive strand convention adopted therein. The long open boxes indicate the positions and extents of the viral genes encoded in the positive strand. Panel B: alkaline denaturing gel analysis following digestion with micrococcal nuclease of DNA extracted from infected cells, to reveal packaged genomes. Southern transfers were probed to detect negative or positive sense strands, with probes 1 or 2, respectively. The left lane, labeled pMVM, contains duplex viral genomes excised from the plasmid pMVMp by digestion with *Aat*II and *Bam*HI, used as a standard for determining the size and concentration of individual packaged strands. Unit length genomes are indicated, as well as a series of deleted forms described further in the text. Relative abundancies of plus and minus strands in each preparation, shown below each lane, were determined relative to the signals in the pMVM lane, which were assumed to contain a 1:1 mixture. Panel C: genomes from the peak fraction of mature virions in an iodixanol gradient, analyzed on denaturing gels as described for panel B, except that samples were either untreated, or digested with proteinase K alone or following micrococcal nuclease digestion, as described in the text. The Southern transfer was probed sequentially with the probes indicated, which hybridize to the strand and nucleotides detailed, and with a stripping step between hybridizations, performed as described in the text. Panel D: predicted secondary structure of the "attenuator" sequence located between nucleotides 292 and 341 of the MVM genome, as proposed by Ben-Asher and Aloni (1984) in viral transcripts originating from the P4 promoter. The sequence shown is that of the positive strand of viral DNA.

Fig. 1B, extracts derived by freezing and thawing MVM-, MML-, and LuIII-infected cells are shown following nuclease digestion (to remove non-encapsidated DNA), electrophoresis through a denaturing agarose gel and Southern transfer. This transfer was then hybridized sequentially with ^{32}P-labeled oligonucleotide probes that detect either negative or positive sense DNA (probes 1 or 2, as shown in Fig. 1A). Control duplex genomes, excised in vitro from an infectious plasmid clone of MVMp using restriction enzymes, were used as a standard for genome size and quantitation. (e.g., Fig. 1B, lane 1). In this analysis, all virion populations were seen to contain some defective,

sub-genomic length DNA(s), which are a characteristic feature of viral stocks propagated in the 324 K cell line used here. While the concentrations of these sub-genomic forms varied somewhat from preparation to preparation, the banding pattern was consistent for any particular genomic sequence. Thus, for example, there were three specific forms of sub-genomic negative-sense MVM DNA, but the largest of these failed to accumulate in the virus MML (Fig. 1B, compare lanes 2 and 3), in which the right-end hairpin of MVM is substituted with that of LuIII. Nevertheless, full-length forms remained the predominant species of negative-sense MVM and MML DNA, but full-length positive-sense MML strands were rare, since >75% of these carried a specific deletion, denoted as δ1 in Fig. 1B (lane 3). A deletion of similar size was also seen in the LuIII population (Fig. 1B, lane 4), where it constituted approximately 20% of the positive-sense DNA, while the majority of these genomes appeared full length.

The MML-infected cell extracts were then sedimented to equilibrium in a gradient of the non-ionic density medium iodixanol and fractions collected from the bottom of the tube. Fig. 1C shows genomes from the peak fraction of mature virions (F5), both before and after digestion with nuclease and/or proteinase K. When probed for negative-sense sequences, this fraction was seen to contain one predominant genome-length species (probe 1, left lane), which migrated slightly faster after proteolysis (probe 1, center lane), presumably as a result of the removal of the NS1 molecule that is covalently-attached to the 5′ end of the packaged strand (Cotmore and Tattersall, 1989). As expected, DNA mobility was not significantly increased further by nuclease-digestion prior to proteolysis (probe 1, compare center and right lanes), indicating that the genome was effectively sequestered within the capsid. We have previously shown that 22–24 nucleotides from the extreme 5′ end of negative-sense MVM DNA, the so-called tether sequence, is exposed on the outside of infectious virions (Cotmore and Tattersall, 1989). However, removal of such a short sequence would not be detected at the resolution of the gels used here. In contrast, when the blot was stripped and re-hybridized with an equivalent probe directed against positive-sense sequences (probe 2), a major genome-length band was again detected (Fig. 1C, probe 2, left lane), which migrated slightly faster following digestion with proteinase K (center lane). However, there was also a trace of the δ1 deleted form mentioned previously, which did not change mobility following protease digestion. Moreover, when these virions were digested with nuclease prior to electrophoresis (probe 2, right lane), approximately 70% of the previously full-length positive-sense DNA was converted to a form that co-migrated with δ1, indicating that while the majority of virions in this fraction were associated with unit-length, 5 kb, single-stranded genomes, several hundred nucleotides of most of these strands remained accessible to nuclease—presumably outside the capsid.

The packaging process falters at a stem–loop structure located near the 5′ end of the positive strand

When packaging complexes were re-probed with sequences that hybridize to the left (5′) end of the positive strand (Fig. 1C, probe 3) only full-length genomes were detected, indicating that the δ1 forms lacked these nucleotides, and hence must lack the entire left-end hairpin. In contrast, a probe that detected the right (3′) end of positive strands hybridized to both unit length and δ1 forms of DNA (Fig. 1C, probe 4, right lane). We then explored the possibility that secondary structure in the packaging strand might play a role in the generation of the δ1 form. Viral DNA and RNA from this end of the genome potentially assume a stem–loop structure, centered around nucleotide 317, as shown in Fig. 1D. This putative structure has been reported to be responsible for the generation of prematurely truncated, "attenuated" P4 transcripts, which terminate at nucleotide 351, although the significance of these small RNAs is currently unknown (Ben-Asher and Aloni, 1984; Perros et al., 1994; Resnekov and Aloni, 1989; Spegelaere et al., 1991). A probe that detected sequences immediately 5′ to this putative attenuation site (Fig. 1C, probe 5) detected full-length genomes and a faint smear of DNA stretching down to, but not including, the δ1 form, whereas probe 6, directed against sequences 3′ to the attenuation site, detected both forms of the genome. This suggests that the packaging mechanism falters when it encounters the beginning of the stem in this secondary structure element, leaving ~350 nucleotides from the 5′ end of the positive strand outside the particle, whose nuclease digestion product is the δ1 form.

Subgenomic positive-sense DNAs between 1 kb and 4 kb long contain sequences derived predominantly from the 3′ end of the strand

Capsid-associated DNAs from less dense fractions of the MML equilibrium gradients were immunoprecipitated with anti-capsid antiserum, both before and after nuclease digestion, and analyzed as before by Southern transfer. For this analysis, the electrophoretic step was shortened so that even severely truncated species remained in the gel, and the resulting transfers were sequentially probed with radiolabeled oligonucleotides that recognized 3′ or 5′ sequences from each strand, as shown in Fig. 2. Some virions with 5 kb genomes trailed through the less-dense fractions, possibly because they were associated with cell fragments containing viral receptors.

Panel A in Fig. 2 shows species that contain sequences from the 3′ (right) end of positive-sense strands (probe 4, shown in Fig. 1A), while panel B shows strands containing sequences from its 5′ end (probe 3). Since these oligonucleotides hybridize once per genome, all molecules containing this sequence bind the probe equally well, and thus signal intensity for each band is proportional to its molarity. Full-length genomes associated with virions that trailed

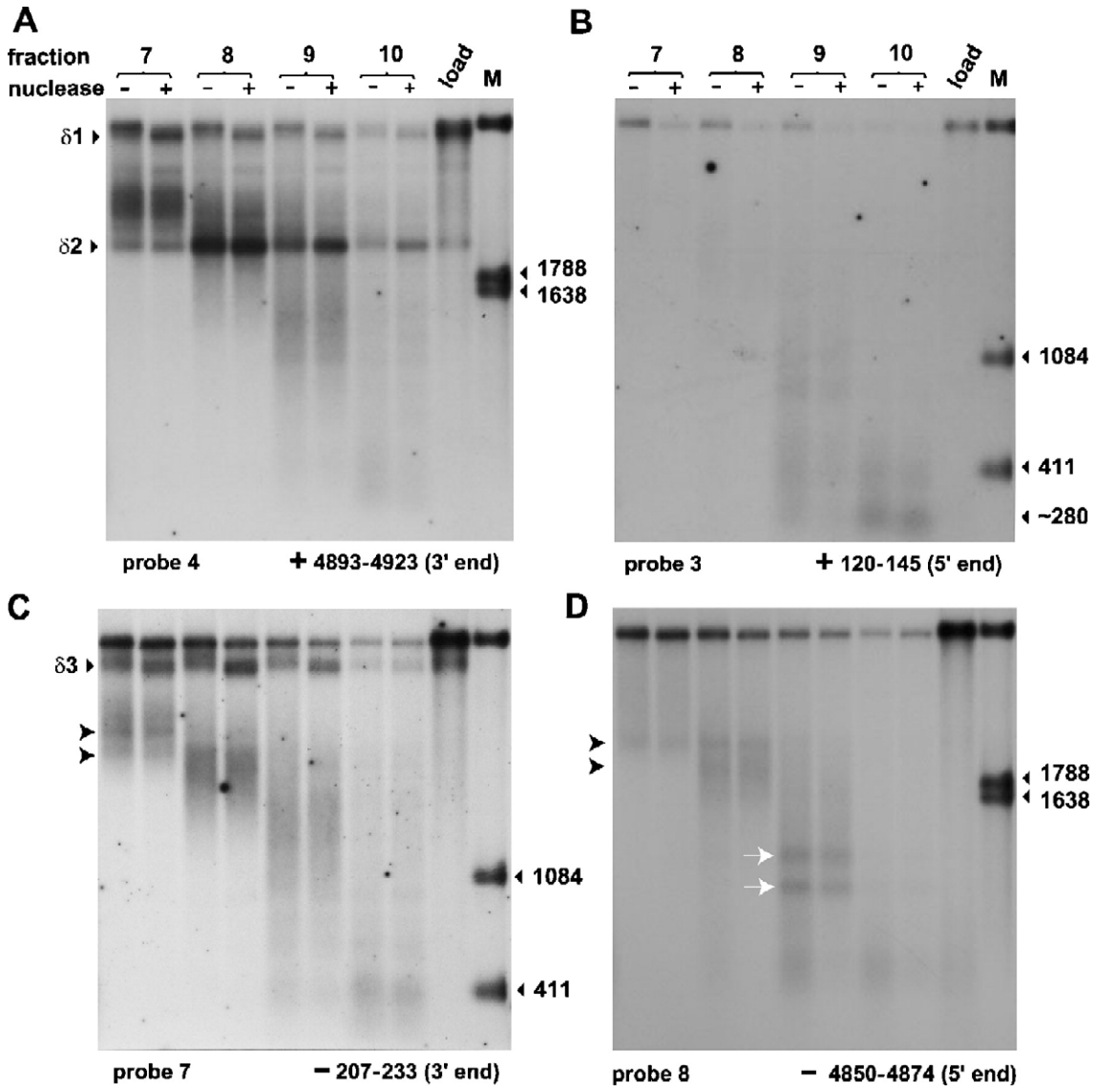

Fig. 2. Identification of partially packaged forms of viral DNA. Viral DNA present in fractions of an iodixanol gradient that banded lighter than mature virions was analyzed by alkaline gel electrophoresis, before and after micrococcal nuclease digestion. DNA on the gel was transferred to nylon and hybridized sequentially with a number of the probes described in Fig. 1. The lane marked "load" contains an undigested sample of the input material for the gradient. "M" denotes the marker lane, which contains a mixture of full-length genomes, excised from pMVMp, and restriction fragments derived from the full-length genome by digestion, separately, with *Pst*I or *Eco*RI, each of which cleave at multiple sites in the viral sequence. The nucleotide lengths of marker fragments detected by each probe are indicated to the left of each panel. In each panel, the bottom of the gradient is toward the left. Panel A: the Southern transfer was hybridized with probe 4, which detects the 3′ end of the plus strand between nucleotides 4893 and 4923. Panel B: the Southern transfer shown in Panel A was stripped and re-hybridized with probe 3, detecting the 5′ end of the plus strand (nucleotides 120–145). Panel C: the Southern transfer shown in Panel B was stripped and re-hybridized with probe 7, which hybridizes to the 3′ end of the minus strand (nucleotides 207–233). Panel D: the Southern transfer shown in Panel C was stripped and re-hybridized with probe 8, hybridizing to the 5′ end of the minus strand (nucleotides 4850–4874).

through these lighter gradient fractions, seen particularly in fractions 7 and 8, generally had ~350 bases from the 5′ end of the DNA exposed at the particle surface, so that nuclease digestion reduced them to the δ1 form described previously. However, the great majority of capsid-associated positive-sense strands in these samples migrated as a highly non-uniform continuum of bands, between ~1 and 4 kb in length, which contained sequences from the 3′-end, but not the 5′-end, of the strand. Forms of around 2 kb predominated in this continuum, and there were many discrete bands, including one major species of around 2.2 kb, designated δ2 in Fig. 2A, which is characterized in more detail below. DNA molecules containing right-end (3′) sequences were observed extending down from 2 kb to ~1.2 kb (Fig. 2A, fraction 9), but their abundance gradually diminishes as they decrease in size, and smaller forms were rare.

In contrast to results obtained with the 3′-end probe, remarkably few positive strand packaging intermediates contained sequences from the 5′ end of this strand (Fig. 2B), suggesting that the type I defective genomes discussed

earlier (Faust and Ward, 1979) were absent from this preparation. The significance of a nuclease-resistant ~280 nucleotide long species seen with the 5′ probe in fraction 10 remains unclear. It is too small to be a type I defective, although it could have the hairpin structure described for type II defectives. If so, it would differ from those described by Faust and Ward in that it must be derived from the left-end, rather than the right-end, of the genome. No bands smaller than 280 nucleotides were observed in these hybridization analyses.

Most of the sub-genomic, capsid-associated positive-sense DNA in these fractions, therefore, comes from the 3′ end of the strand, and must either correspond to type II defective genomes or represent partially translocated DNA strands in the process of being encapsidated in a 3′- to-5′ direction, as reported for AAV2 by King et al. (2001). Nuclease digestion appeared to have little effect on the mobility of most discrete species in this continuum. However, the virus preparation was generated using a freeze/thaw lysis procedure that would inevitably release nucleases, suggesting that most complexes with long stretches of exposed DNA are likely to have been nicked during isolation. Further nuclease digestion did conspicuously enhance specific bands in certain fractions, such as the δ2 form in fractions 9 and 10, suggesting that virions in these fractions were associated with significant stretches of non-internalized DNA.

Although comparison of fractions 9 and 10 before and after nuclease digestion suggests that the exposed DNA is probably only a few hundred nucleotides in length, it apparently lowers the density of the virions, causing them to band higher up the gradient than the bulk of δ2 forms (see fraction 8). Removal of short residual exposed sequences would not be detected at this gel resolution, but a large molar excess of empty viral particles peaked in fraction 8, as determined by the gradient's hemagglutination profile (data not shown), at the same density as the major peak of δ2 forms, even though the latter contained ~2.2 kb of internalized DNA. This suggests that most members of the δ2 species band somewhat anomalously in the gradient, possibly because they all retain at least some exposed DNA.

We therefore conclude that positive-sense MML DNA readily associates with MVM capsids, and the first 1 kb to 2 kb from its 3′ end is efficiently translocated into the particle, but mechanisms responsible for internalizing the rest of the strand are inefficient, and routinely pause or terminate prematurely at a number of discrete sites.

The 1 kb to 3 kb smear of negative-sense DNA also contains sequences derived predominantly from the 3′ end of the strand

Panel C in Fig. 2 shows the distribution of sequences from the 3′ (right) end of negative-sense DNA (probe 7, shown in Fig. 1A), while panel D shows species reacting with the minus-sense 5′ probe (probe 8). Once again, a continuum of sub-genomic species was observed with the 3′ probe, ranging from ~1 to 3 kb in length, with species of around 2 kb predominating. However, these forms were less abundant than their positive-sense counterparts, accounting for approximately one fifth of the total DNA between 1 and 4 kb in this gel as assessed, relative to standards, by phosphor-imager analysis. Moreover, the continuum of forms was much more uniform, lacking specific dominant forms like the δ2 deletion seen for the positive-strand. By analogy with the positive-sense DNA, we suggest that this smear may represent a series of partially internalized progeny strands, although in this case nuclease digestion revealed little evidence of exposed DNA. In contrast, nuclease digestion did reveal a doublet of partially internalized DNAs of ~4 kb that lacked sequences from the 5′ end of the genome (dubbed δ3 in Fig. 2, cf. panels C and D), which were observed previously as minor constituents in the unfractionated MML preparation (Fig. 1B, lane 3) but were not present in the peak fraction from this gradient (shown in Fig. 1C). The existence of these forms suggests that, even when derived from negative-sense DNA, sequences from the extreme 5′ end of the strand may cause the translocation machinery to falter. Forms smaller than 1 kb were again rare, the exception being a diffuse band of around 400 nucleotides seen in fraction 10, which corresponded to a faint band seen with the positive-sense 5′ probe in panel B, and so may represent a hairpin form of the left-end. There was minimal, if any, evidence of molecules of around 290 bases, which would correspond to forms in which the strand translocation machinery had stalled at the beginning of the negative strand equivalent of the "attenuator" stem–loop structure discussed previously. Thus, while the stem–loop illustrated in Fig. 1D presents an almost insuperable problem for the packaging machinery if it is encountered at the 5′ end of the positive-sense strand, at the 3′ end of the negative strand, its inverse complement appears to have little impact on encapsidation.

DNA species derived from the 5′ end of the negative strand were more abundant than their positive-sense counterparts (Fig. 2, cf. panels B and D), and sometimes formed discrete bands, which we suggest may be dominant forms of the previously described defective genomes. Some of these, denoted by black arrowheads in fractions 7 and 8, appear to represent type I defectives, since they correspond to minor species seen at similar molarity with the 3′ probe. The two discrete bands of ~1 kb and 1.2 kb, denoted by white arrowheads in fraction 9, do not correspond to DNA species carrying 3′ sequences, and are candidates for type II defectives, that is, palindromic molecules, carrying two copies of the right end palindrome at both the 3′ and 5′ end of the strand. In general, we conclude that defective genomes of the types described by Faust and Ward (1979) are present, but are less abundant

than authentic packaging intermediates in infections such as these, which were initiated with virus stocks derived by expansion from low input multiplicity.

Differential probing of negative-sense strands provides evidence for the limited accumulation of a continuum of 3′ enriched forms, 1–3 kb in length, that somewhat resembles the pattern seen for positive-sense DNA, and is compatible with the notion of vectorial encapsidation in a 3′- to-5′ direction. However, by itself, these data are not compelling, since packaging intermediates involving negative-sense strands may simply fail to accumulate to similar levels in vivo because this strand is internalized more efficiently. Thus, we suggest that negative-sense MVM genomes are constantly exposed to selective pressure, resulting in the evolution of forms that are optimally compatible with the packaging mechanism. In contrast, there has been no such selection operating on the plus strand, and it contains a number of sequence elements scattered throughout the 5′ two thirds of the strand that cause the translocation machinery to pause or terminate prematurely. Significantly, while more extreme for plus strands, even minus strands show some evidence of premature termination near their extreme 5′ ends, suggesting that internalizing the last few hundred nucleotides can present particular problems for the translocation machinery.

A G-rich sequence causes positive strand packaging to terminate 2.24 kb from its 3′ end, generating the δ2 deletion

We were particularly interested to discover what sequence in the positive-sense strand might cause packaging to terminate so routinely that it gives rise to the major deleted form δ2 observed in Fig. 2A. To explore this further, we generated new MML-infected cell extracts, this time scraping the cells into extraction buffer containing 5 mM EDTA, to chelate calcium ions and hence impede endogenous nuclease activity. After three successive rounds of freezing and thawing, extracts were centrifuged and the supernatant and pellet fractions analyzed separately. These samples are shown in Fig. 3, before and after nuclease digestion. When probed for sequences from the 3′ end of the plus strand (probe 4, shown in Fig. 3A), similar spectra of nuclease resistant DNAs, including the δ1 and δ2 deletions, were present in both the viral extract and the residual cell pellet

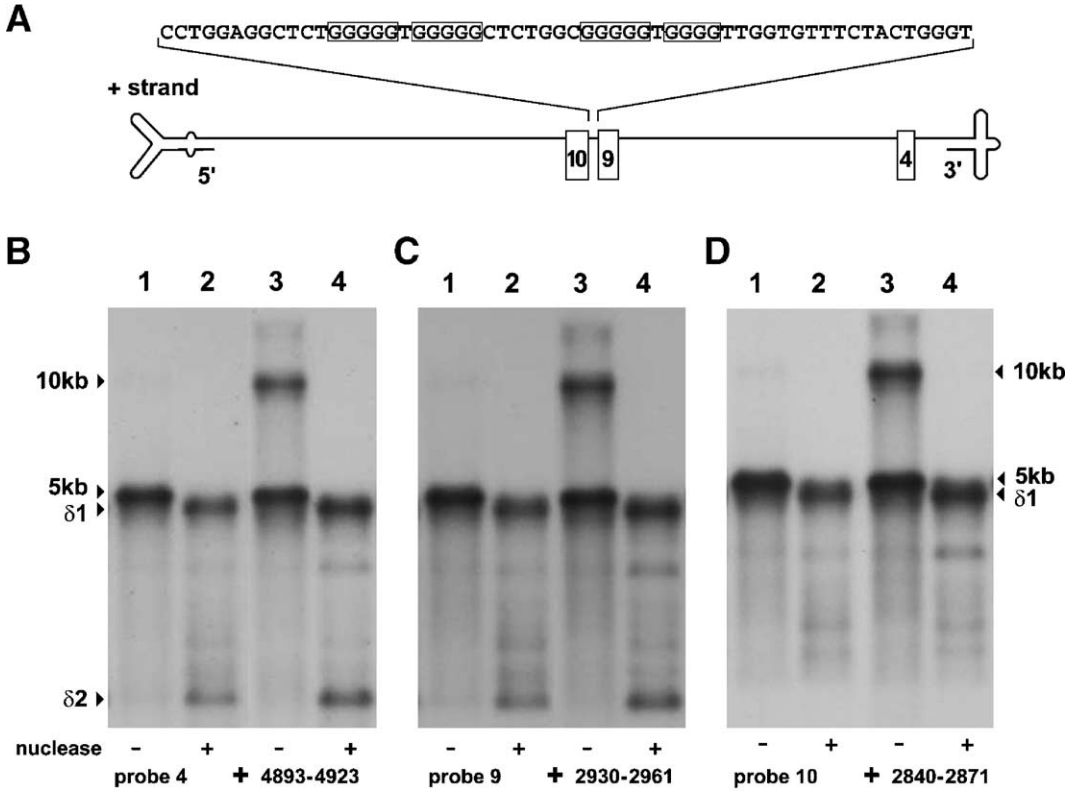

Fig. 3. Mapping of the major pause site that generates the δ2 deletion. Panel A: diagram of the MML genome showing the locations of probes 9 and 10, which hybridize to nucleotides 2930–2961 and nucleotides 2840–2871, respectively, on the positive strand. Shown expanded above the positive strand is the G-rich sequence between nucleotides 2873 and 2931 that is discussed in the text. Blocks of four or more consecutive G residues are boxed. Panel B: MML-infected cells were extracted in buffer containing 10 mM EDTA and centrifuged. The supernatant fraction (lanes 1 and 2) and pellet fraction (lanes 3 and 4) were then analyzed separately on an alkaline denaturing gel, both with and without prior micrococcal nuclease digestion, as indicated below each lane. The Southern transfer was hybridized with probe 4 (described in Fig. 1). Panel C: the Southern transfer shown in Panel B was stripped and re-hybridized with probe 9 (described in Panel A). Panel D: the Southern transfer shown in Panel C was stripped and re-hybridized with probe 10 (described in Panel A). Images presented here were truncated to focus on the region of the gel containing the δ2 deletion.

(Panel B, lanes 2 and 4, respectively). Prior to nuclease treatment, viral supernatants contained predominantly genome length (5 kb) DNA (lane 1), while residual pellets contained both 5 kb DNA and 10 kb replicative-form DNAs (lane 3), indicating that the δ1 and δ2 forms seen in lanes 2 and 4 were generated by digestion of unprotected DNA sequences from intermediates that originally contained genome-length DNA.

The blot shown in panel B was then stripped and re-probed with additional labeled oligonucleotides, in order to determine where the δ2 deletion terminated. As seen in Fig. 3 (Panel C), probe 9 identified the same forms of positive-strand DNA in this part of the gel as probe 4, while probe 10 specifically failed to detect the δ2 form (Fig. 3, panel D). Thus, the δ2 deletion resulted from the inability of the translocation machinery to internalize sequences between nucleotides 2929 and 2872 (shown in Fig. 3A), which is a guanidine-rich region that contains four guanidine tetra- or pent-nucleotides.

Amino-terminal peptides from VP2 are exposed at the exterior of all particles containing partially packaged genomes

MVM particles are made up from 60 copies of a core C-terminal polypeptide sequence that is shared by all capsid proteins. Approximately 50 of these are derived from VP2 molecules, while the rest are contributed by the VP1 polypeptide, which is 142 amino acids longer than VP2 at its N-terminus. In the atomic model of the MVM virion, 547 carboxy-terminal amino-acids from these proteins are icosahedrally ordered, so that just 38 residues from the VP2 amino-termini do not contribute defined density following rotational averaging (Agbandje-McKenna et al., 1998). In the crystal structure, narrow pores penetrate through the capsid shell to the particle interior at each of the twelve 5-fold symmetry axes, and VP2 residue 40 lies on the inside of the shell, at the base of these channels. In mature virions, but not in empty viral particles, these pores contain additional, weak, X-ray-dense material into which can be modeled the highly-conserved glycine-rich sequence that extends from residues 28–38 in VP2. Thus, at any one time, the first 28 residues of one in every five VP2 N-termini appear to be exposed at the particle exterior in full virions, where they are accessible to antibodies, proteases and, presumably, cellular ligands. These amino terminal peptides, which are sequestered within empty particles, seem to act as viral "luggage tags", creating an unusual phosphoserine-rich nuclear export motif that allows full virions, but not empty particles, to be exported from the nucleus and subsequently released from the host cell prior to lysis (Maroto et al., 2004).

To this point, we had assumed that these amino-terminal peptides are extruded in response to pressure generated within the particle as the genome is introduced (Cotmore et al., 1999). However, the accumulation of partially packaged virions in MML infections presents an opportunity to explore this hypothesis and, if correct, to determine exactly how much internalized DNA is required to induce peptide extrusion. For this, we treated MML-infected cultures with neuraminidase in order to destroy the virus receptor and ensure the removal of all virus that was not actually inside the cells, then washed and harvested the resulting monolayers. Cell pellets were disrupted by sonication in SDS-containing "RIPA" buffer at 4 °C, and samples immunoprecipitated with specific antisera. These immunocomplexes were then digested with micrococcal nuclease and proteinase K, electrophoresed through denaturing gels, transferred to nylon and probed separately for 3′ sequences from each strand. Antibodies directed against intact viral particles quantitatively precipitated partial encapsidation products, derived from either strand, ranging in size down to approximately 1 kb, and including the 2.24-kb δ2 positive-strand deletion product, as shown in Fig. 4 (lane 3 in each panel). Importantly, these partially packaged complexes were also precipitated by antibodies raised against the extreme amino-terminal peptide of VP2 (lane 4) so completely as to leave no residual virion DNA in the unbound material (lane 6). None of these forms were precipitated with pre-immune serum (lane 5). Thus, extrusion of the VP2 N-termini to the particle surface substantially precedes translocation of the full-length strand.

Discussion

The packaging substrate is a free single strand

In this paper, we characterize packaging complexes generated in vivo when the right-end hairpin of MVM is replaced with that of LuIII, creating MML, a chimeric virus that encapsidates both plus and minus strands. While packaging of positive-sense DNA by this virus begins efficiently, it rarely goes to completion, apparently because the translocation machinery falters when it encounters specific sequence configurations, which are either not present or not a problem, when encountered in MVM's authentic negative-sense substrate. This has allowed us to isolate an abundance of paused packaging intermediates. Analysis of their partially packaged, positive-sense genomes reveals that they contain pre-excised and displaced 5 kb single-strands, which have been partially translocated in a 3′- to-5′ direction into pre-formed MVM particles, as described previously for AAV-2 (King et al., 2001).

Prior to nuclease-digestion, most positive-sense DNAs in virion fractions were unit-length genomes, suggesting that the substrate for encapsidation is a pre-excised, displaced, 5 kb single strand, rather than one strand of a replicative form (RF) DNA molecule, since packaging by displacement from RF molecules would lead to half of the DNA associated with these particles appearing as fully nuclease-sensitive strands. The same argument also suggests that the packaging

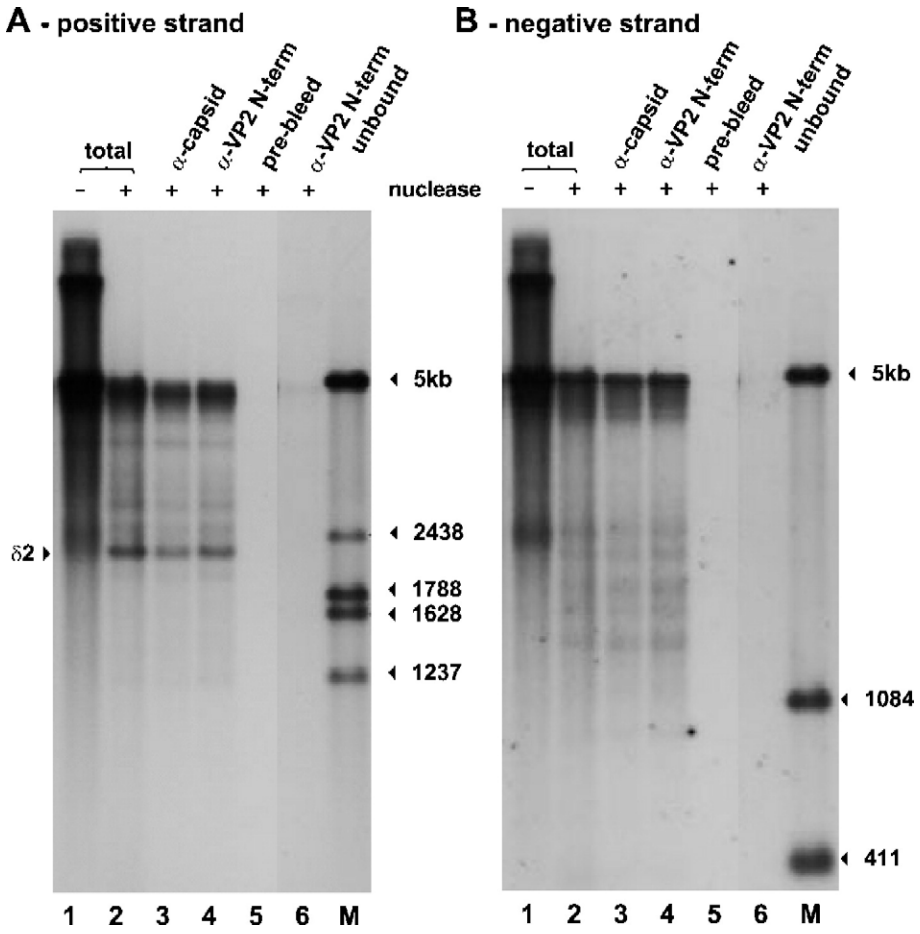

Fig. 4. Immunoprecipitation analysis of packaging complexes. MML-infected cell pellets were disrupted by sonication in "RIPA" buffer as described in the text, and samples immuno-precipitated with specific antisera described elsewhere (Cotmore et al., 1999). Lanes 1 and 2 contain extract before (lane 1) and after (lane 2) digestion with micrococcal nuclease. Lane 3 contains extract precipitated with α-capsid antibody, a rabbit antiserum specific for intact capsids. Lane 4 contains extract precipitated with α-VP2 N-term, a rabbit antibody raised against the first 12 residues of VP2. Lane 5 contains material precipitated by the pre-immune serum from this rabbit, and lane 6 contains the non-precipitated material from lane 4. Immunocomplexes were digested with micrococcal nuclease and proteinase K, then analyzed, as before, by denaturing gel electrophoresis followed by Southern transfer to a nylon membrane. Panel A: the transfer was hybridized with a mixture of probes 4 and 9, in order to detect 3′ sequences of positive strands. Panel B: the membrane was stripped and re-hybridized with probe 7, which detects negative strand 3′ sequences.

substrate is not a partially released single strand that has been cleaved at its 3′ or 5′ end, but is awaiting resolution of its second telomere. Thus, MVM does not appear to employ a particle-associated, terminase-like cleavage mechanism, where the packaging substrate is cleaved following the introduction of a complete genome into the particle, as is the case with other viruses that package linear DNA genomes (Catalano, 2000; Yu and Weller, 1998). Rather, our results imply that both the 3′ - and 5′ -termini of a progeny strand are available to interact with the packaging machinery before encapsidation initiates.

In contrast to our findings for the positive strand, minus-sense DNA appears to be encapsidated relatively efficiently, so that partially internalized 3′ forms of this strand accumulate to much lower levels. Following nuclease-treatment, packaging complexes containing these negative-sense strands gave rise to an almost uniform continuum of DNA species ranging from 1 to 3 kb in length, while those containing positive-sense DNA showed an additional non-uniform spectrum of products superimposed on this smear, with major distinct species that ranged from around 2–5 kb. This suggests that the translocation mechanism rarely encounters specific "problem" sequences in negative-sense DNA, at least until it nears the extreme 5′ end of the strand, although it still tends to pause or terminate prematurely at random sites after 1–3 kb of DNA has been internalized.

Packaging of either strand is a biphasic process

At present, we do not know if the partially packaged forms we have identified accumulate because the translocation mechanism simply slows after the first 1–2 kb of each strand has been internalized, or if the process then becomes prone to premature termination, or both. In either case, their presence suggests that there are two distinct phases in the internalization process, an initial period, characterized by the relative scarcity of intermediates in which less than 2 kb has been internalized, and during which packaging proceeds effi-

ciently, followed by a slower, or perhaps discontinuous, second phase during which the residual 2–5 kb is encapsidated. In the present study, this second phase, involving the 5′ half of each strand, is seen to be highly vulnerable to interruption by structured elements in the DNA, but evidence for some sort of "change in gears" part way through the process also derives from the smooth continuum of forms seen for this region of negative-sense DNA.

What drives packaging?

King et al. (2001) observed a somewhat similar biphasic pattern of genome internalization for AAV2, involving an efficient first step, during which 50–75% of the strand was encapsidated, followed by the accumulation of a diffuse band of partially protected intermediates, spanning the remaining ~2 kb of the genome (King et al., 2001). These authors also observed a third diffuse smear of low molecular DNA, which we did not detect, that was derived from internal genomic locations, since it hybridized to a random-primed probe spanning AAV-2 nucleotides 683–2411. The diffuse ~2 kb band of partially internalized AAV-2 DNAs accumulated even in the absence of active forms of the small Rep helicases (King et al., 2001), suggesting either that translocation of the DNA to this point does not require effective helicase activity, or that large Rep molecules can substitute for the small Reps during this phase of internalization. The crystal structure of Rep40 has been determined (James et al., 2003), and by analogy with SV40 T antigen has been modeled as a hexameric ring. In this model, peptide loops carrying residues K404 and K406, which are essential for single-strand DNA binding, project into a central pore, 18A in diameter, through which the single strand would pass during the process of DNA unwinding or strand translocation (Yoon-Robarts et al., 2004). However, these two lysine residues, which are conserved across the entire family *Parvoviridae*, and have been shown to be essential for strand translocation, could also potentially function by facilitating interactions within a dimeric form of the helicase, so that at present we have little concrete information about the structure of the parvoviral packaging motor or how it interacts with any putative portal in the capsid. Like their AAV counterparts, MVM strands presumably require a highly organized motor to accomplish strand translocation, and we expect that this motor is derived from the 3′-to-5′ helicase domain of MVM NS1, but we do not currently know what form such molecules take, or how they are generated.

Capsid: DNA interactions as an additional catalyst of packaging

Difference electron-density maps, derived by comparing X-ray crystallographic data from MVMi virions and empty particles, show that just over a third of the viral DNA exhibits some level of icosahedral symmetry within the particle (Agbandje-McKenna et al., 1998). This symmetry, which involves 29 nucleotides per icosahedral asymmetric unit, reflects the interaction of bases in the genomic single strand with side chains of amino acids lining the inner surface of the capsid. Thus, a significant proportion of the outermost layer of packaged DNA has an unusual loop conformation, with its bases hydrogen bonded to side chains from the capsid amino acids, while its phosphate groups, surrounding metal counterions, face towards the particle interior. The most ordered part of this density was first observed in CPV virions, where it corresponds to 11 nucleotides per asymmetric unit, which make 15 putative hydrogen bonds with capsid amino acids (Chapman and Rossmann, 1995). These interactions are highly conserved in MVM, so that they effectively identify an icosahedrally repeated DNA recognition domain on the capsid interior. In CPV, analysis of the DNA electron-density indicated preferences for particular bases in parts of this binding site, allowing a weak consensus sequence to be derived that corresponds to about 60 thymidine-rich sequences of 11 nucleotides in the CPV genome. Thus, optimal packaging or virion stability may require, or be facilitated by, reiterations of certain types of degenerate, thymidine-rich motifs in the viral chromosome, which form intimate contacts with residues lining the capsid shell. Since favorable interactions of this type might diminish the energy barrier resisting strand translocation, and might even create an energy "sink" that would promote strand internalization, it is possible that the facility with which the first 3′ third of the DNA stand is internalized reflects occupation of these capsid motifs, which consequently offers little resistance to the packaging machinery.

An alternate, or perhaps complementary, explanation for the two phases of packaging is suggested by analogy to studies of energy consumption during double-stranded DNA translocation by the bacteriophage ϕ29 (Smith et al., 2001). Single molecule measurements using "optical tweezers" have shown that this packaging reaction is also biphasic, with internalization of the first half of the genome requiring little energy, while translocation of the second half demands the expenditure of increasing amounts of ATP. Finally, the phage's packaging motor stalls out after internalizing DNA corresponding to approximately 106% of its genome length, indicating that this motor has evolved to be just strong enough to package a whole genome effectively. While this analogy may in some ways be extrapolated to the problem of parvoviral strand translocation, it should be emphasized that the phage's double-strand DNA genome is far more rigid, and would resist compression in a way that would not be expected of single strand DNA.

The onset of packaging triggers reconfiguration of the viral capsid

VP2 amino-terminal peptides are not exposed at the surface of empty MVM particles (Cotmore et al., 1999; Reguera et al., 2004; Tattersall et al., 1977), but are accessible

in the putative packaging intermediates analyzed herein, indicating that these peptides had already been extruded from the particle interior through the 5-fold pores. It has previously been suggested that extrusion of these peptides might result from internal pressure exerted by the tight-packing of viral DNA into the particle (Cotmore et al., 1999), but their exposure on these "early" intermediates suggest this interpretation is incorrect. Instead, it appears that VP2 extrusion either closely follows the translocation of 3′ terminal DNA sequences into the particle, or accompanies the assembly of an as yet unidentified portal structure prior to strand internalization. Thus, it is possible that the first DNA to enter the capsid represents the structured outer sphere of polynucleotides within the particle, and that the interactions between the bases of this DNA layer and the inside surface of the capsid are strong enough to exert the pressure required to extrude the bulky, phosphorylated VP2 amino-termini. Alternatively, or perhaps concomitantly, interaction between the packaging machinery and the capsid could cause a structural transition in the empty shell that opens each pore, allowing extrusion of the VP2 amino-terminal peptide. In this model, the pores then re-close around residues 28–38 in the VP2 chain, containing the glycine-rich sequence, to generate a structure that presumably represents the lowest free-energy state. Thus, extrusion of the VP2 amino-termini might provide a mechanism for sealing these pores prior to translocation of the bulk of the genome, against increasing internal pressure, into the capsid interior.

Packaged strand sequence is under selective pressure at the structural level

Finally, the current observations suggest that for viruses that package predominantly a single-sense strand, selective pressure is exerted on that strand to minimize the presence of ill-suited elements, such as stem–loop configurations and reiterated G_4 clusters, thus, ensuring optimal compatibility with the translocation machinery. This type of G-rich sequence can adopt complex, stable secondary structures, including Hoogsteen base-paired G-quartet configurations that can interact with one another (Kim et al., 1991; Raghuraman and Cech, 1990). Thus, it appears that the translocation mechanism falters when required to process sequences within the DNA strand that are capable of adopting stable secondary structures. An analysis of parvoviral genomes for homopolymeric nucleotide runs of N_4 or greater tends to support this conclusion. In viruses from the *Amdovirus*, *Parvovirus*, and *Bocavirus* genera (Tattersall et al., 2005), which package predominantly the negative strand, stretches of G_4 or longer are either entirely absent from the minus strand or under-represented by more than 10-fold compared to the plus strand. Thus, for example, the negative-sense single-stranded regions of AMDV, MVM, H1, KRV, FPV, and BPV are entirely devoid of such G tetrads, whereas their equivalent positive-sense sequences contain 20, 14, 15, 19, 21, and 49 G_4 clusters, respectively. Likewise, while MPV and CnMV each have a single G4 element in the coding region of their negative strands, the equivalent region of their positive strands contain 15 and 23 of these sequence blocks, respectively. In contrast, for viruses from the *Dependovirus* and *Erythrovirus* genera, which package either strand with equal efficiency, such runs of G are equally represented on both strands. Indeed, in these viruses, such sequences do not even appear to be specifically restricted, since AAV2 has 20 and 14 such sequences on its negative- and positive-sense strands, respectively, while the *Erythrovirus* B19(Au) has 32 and 33. Whether or not this indicates differences in the packaging motors employed by different genera remains to be determined, but it would be interesting to know how efficiently MVM and AAV might package each others genome. Viruses from both the *Dependovirus* and *Parvovirus* genera are currently receiving attention as potential experimental and therapeutic gene transfer vectors, since they allow the efficient delivery of foreign genes to a wide range of mammalian cells (Buning et al., 2004; Cornelis et al., 2004). However, yields of such vectors constructed from species within the *Parvoviruses* are often disappointingly low. The observations presented here provide one potential explanation for this phenomenon and suggest that minimizing regions of potential secondary structure in the transgene sequence may well enhance vector yield.

Materials and methods

Viruses and cells

The chimeric virus MML was described previously (Cotmore and Tattersall, 2005). Briefly, it is based on the prototype strain of MVM (MVMp), but has the right-end hairpin of LuIII, exchanged around a *Psh*I site at MVM nucleotide 4912. MML and its parent viruses were propagated in the SV40-transformed human kidney cell line, 324 K, maintained in DMEM supplemented with 5% fetal bovine serum. For immuno-precipitation studies, *Clostridium perfringens* neuraminidase (0.05 U/ml) was added to the medium of infected cells 8 h prior to harvest, to prevent further virus uptake and allow subsequent removal all non-internalized virions.

Virus extraction and fractionation on iodixanol gradients

Viral stocks were derived by transfection of 5×10^5 324 k cells with 2 μg of an infectious plasmid clone using Superfect (Quiagen, Valencia, CA). Cells were expanded until they exhibited the first sign of viral cytotoxicity, and then harvested by scraping. After centrifugation, pellets were resuspended in 50 mM Tris–HCl, pH 8.7/0.5 mM EDTA (TE8.7), and virus extracted by three cycles of freezing and thawing, followed by centrifugation at 12,000 RPM for 30 min to remove the cell residue. Where specified this

procedure was slightly modified to limit nuclease-digestion of partially packaged DNAs. In this case, cells were rinsed in phosphate buffered saline pH 7.2 (PBS) containing 5 mm EDTA prior to harvest, harvested in the same buffer, and pellets resuspended in TE8.7 containing 5 mm EDTA. Virus was fractionated by centrifugation through step gradients of iodixanol dissolved in PBS (containing 1 ml of 55%, 1.5 ml of 45%, 1.5 ml of 35% and 2 ml of 15% iodixanol), at 18 °C and 35 k for >16 h. Fractions were collected from the bottom of the tube and capsids located by their ability to hemagglutinate guinea pig erythrocytes.

Sample processing, electrophoresis, and Southern transfer

Unless otherwise specified, prior to electrophoresis samples were digested with micrococcal nuclease (50 μg/ml) for 30 min at 37 °C in 50 mM Tris–HCl pH 8.0 adjusted to a final concentration of 5 mM $CaCl_2$. EDTA was then added to 20 mM, and samples further incubated with 100 μg/ml proteinase K at 37 °C for 30 min, before SDS was added to 0.5% and incubation continued for a further 15 min. After addition of NaOH to 0.3 M, samples were analyzed by electrophoresis through 1.4% agarose–0.03 M NaOH denaturing gels. Extracts for immuno-precipitation were predigested with micrococcal nuclease, diluted into RIPA buffer (50 mM Tris–HCl pH 7.5, 150 mM NaCl, 1% NP40, 1% sodium deoxycholate, 0.1% sodium dodecyl sulfate, and 2 mM EDTA), precipitated and processed as described by Li et al. (1994).

Following electrophoresis, gels were transferred to Zeta-Probe GT membranes (Bio-Rad Laboratories, Hercules, CA), DNA cross-linked by UV irradiation, membranes preblocked by incubation at 50 °C in 0.25 M sodium phosphate pH 7.2 containing 7% SDS for 1 h and hybridized overnight under similar conditions with ^{32}P-5′-labeled oligonucleotide probes. After sequential washing at 50 °C for 30 min each in 20 mM phosphate buffer containing first 5% and then 1% SDS, DNA was detected by autoradiography or quantified using a Molecular Dynamics PhosphorImager SI. Membranes were stripped prior to re-probing by incubation in 2 changes of 0.1 × SSC/0.5% SDS for 30 min each at 60 °C.

Acknowledgments

We thank other members of our laboratory, particularly Glen Farr, for many valuable discussions. This work was supported by Public Health Service grants AI26109 and CA29303 from the National Institutes of Health.

References

Agbandje-McKenna, M., Llamas-Saiz, A.L., Wang, F., Tattersall, P., Rossmann, M.G., 1998. Functional implications of the structure of the murine parvovirus, minute virus of mice. Structure 6 (11), 1369–1381.

Ben-Asher, E., Aloni, Y., 1984. Transcription of minute virus of mice, an autonomous parvovirus, may be regulated by attenuation. J. Virol. 52 (1), 266–276.

Buning, H., Braun-Falco, M., Hallek, M., 2004. Progress in the use of adeno-associated viral vectors for gene therapy. Cells Tissues Organs 177 (3), 139–150.

Catalano, C.E., 2000. The terminase enzyme from bacteriophage lambda: a DNA-packaging machine. Cell Mol. Life Sci. 57 (1), 128–148.

Chapman, M.S., Rossmann, M.G., 1995. Single-stranded DNA–protein interactions in canine parvovirus. Structure 3 (2), 151–162.

Chejanovsky, N., Carter, B.J., 1989. Mutagenesis of an AUG codon in the adeno-associated virus rep gene: effects on viral DNA replication. Virology 173 (1), 120–128.

Chen, K.C., Tyson, J.J., Lederman, M., Stout, E.R., Bates, R.C., 1989. A kinetic hairpin transfer model for parvoviral DNA replication. J. Mol. Biol. 208 (2), 283–296.

Christensen, J., Tattersall, P., 2002. Parvovirus initiator protein NS1 and RPA coordinate replication fork progression in a reconstituted DNA replication system. J. Virol. 76 (13), 6518–6531.

Cornelis, J.J., Lang, S.I., Stroh-Dege, A.Y., Balboni, G., Dinsart, C., Rommelaere, J., 2004. Cancer gene therapy through autonomous parvovirus-mediated gene transfer. Curr. Gene Ther. 4 (3), 249–261.

Cotmore, S.F., Tattersall, P., 1989. A genome-linked copy of the NS-1 polypeptide is located on the outside of infectious parvovirus particles. J. Virol. 63 (9), 3902–3911.

Cotmore, S.F., Tattersall, P., 1995. DNA replication in the autonomous parvoviruses. Semin. Virol. 6, 271–281.

Cotmore, S.F., Tattersall, P., 2005. Packaging sense is controlled by the efficiency of the nick site in the right-end replication origin of parvoviruses MVM and LuIII. J. Virol. 79 (4), 2287–2300.

Cotmore, S.F., D'Abramo Jr., A.M., Ticknor, C.M., Tattersall, P., 1999. Controlled conformational transitions in the MVM virion expose the VP1 N-terminus and viral genome without particle disassembly. Virology 254 (1), 169–181.

Faust, E.A., Ward, D.C., 1979. Incomplete genomes of the parvovirus minute virus of mice: selective conservation of genome termini, including the origin for DNA replication. J. Virol. 32 (1), 276–292.

Gorbalenya, A.E., Koonin, E.V., Wolf, Y.I., 1990. A new superfamily of putative NTP-binding domains encoded by genomes of small DNA and RNA viruses. FEBS Lett. 262 (1), 145–148.

Hickman, A.B., Ronning, D.R., Perez, Z.N., Kotin, R.M., Dyda, F., 2004. The nuclease domain of adeno-associated virus rep coordinates replication initiation using two distinct DNA recognition interfaces. Mol. Cell 13 (3), 403–414.

Iyer, L.M., Leipe, D.D., Koonin, E.V., Aravind, L., 2004. Evolutionary history and higher order classification of AAA+ ATPases. J. Struct. Biol. 146 (1–2), 11–31.

James, J.A., Escalante, C.R., Yoon-Robarts, M., Edwards, T.A., Linden, R.M., Aggarwal, A.K., 2003. Crystal structure of the SF3 helicase from adeno-associated virus type 2. Structure 11 (8), 1025–1035.

Kim, J., Cheong, C., Moore, P.B., 1991. Tetramerization of an RNA oligonucleotide containing a GGGG sequence. Nature 351 (6324), 331–332.

King, J.A., Dubielzig, R., Grimm, D., Kleinschmidt, J.A., 2001. DNA helicase-mediated packaging of adeno-associated virus type 2 genomes into preformed capsids. EMBO J. 20 (12), 3282–3291.

Koonin, E.V., Ilyina, T.V., 1993. Computer-assisted dissection of rolling circle DNA replication. Biosystems 30 (1–3), 241–268.

Li, Q., Yafal, A.G., Lee, Y.M., Hogle, J., Chow, M., 1994. Poliovirus neutralization by antibodies to internal epitopes of VP4 and VP1 results from reversible exposure of these sequences at physiological temperature. J. Virol. 68 (6), 3965–3970.

Maroto, B., Valle, N., Rainer, S., Almendral, J.M., 2004. Nuclear export of the non-enveloped parvovirus virion is directed by an unordered protein signal exposed on the capsid surface. J. Virol. 78 (19), 10685–10694.

Myers, M.W., Carter, B.J., 1980. Assembly of adeno-associated virus. Virology 102 (1), 71–82.

Nuesch, J.P., Cotmore, S.F., Tattersall, P., 1995. Sequence motifs in the replicator protein of parvovirus MVM essential for nicking and covalent attachment to the viral origin: identification of the linking tyrosine. Virology 209 (1), 122–135.

Perros, M., Spegelaere, P., Dupont, F., Vanacker, J.M., Rommelaere, J., 1994. Cruciform structure of a DNA motif of parvovirus minute virus of mice (prototype strain) involved in the attenuation of gene expression. J. Gen. Virol. 75 (10), 2645–2653.

Raghuraman, M.K., Cech, T.R., 1990. Effect of monovalent cation-induced telomeric DNA structure on the binding of Oxytricha telomeric protein. Nucleic Acids Res. 18 (15), 4543–4552.

Reguera, J., Carreira, A., Riolobos, L., Almendral, J.M., Mateu, M.G., 2004. Role of interfacial amino acid residues in assembly, stability, and conformation of a spherical virus capsid. Proc. Natl. Acad. Sci. U.S.A. 101 (9), 2724–2729.

Resnekov, O., Aloni, Y., 1989. RNA polymerase II is capable of pausing and prematurely terminating transcription at a precise location in vivo and in vitro. Proc. Natl. Acad. Sci. U.S.A. 86 (1), 12–16.

Richards, R., Linser, P., Armentrout, R.W., 1977. Kinetics of assembly of a parvovirus, minute virus of mice, in synchronized rat brain cells. J. Virol. 22 (3), 778–793.

Smith, D.E., Tans, S.J., Smith, S.B., Grimes, S., Anderson, D.L., Bustamante, C., 2001. The bacteriophage ϕ29 portal motor can package DNA against a large internal force. Nature 413 (6857), 748–752.

Spegelaere, P., van Hille, B., Spruyt, N., Faisst, S., Cornelis, J.J., Rommelaere, J., 1991. Initiation of transcription from the minute virus of mice P4 promoter is stimulated in rat cells expressing a c-Ha-ras oncogene. J. Virol. 65 (9), 4919–4928.

Tattersall, P., Shatkin, A.J., Ward, D.C., 1977. Sequence homology between the structural polypeptides of minute virus of mice. J. Mol. Biol. 111 (4), 375–394.

Tattersall, P., Bergoin, M., Bloom, M.E., Brown, K.E., Linden, R.M., Muzyczka, N., Parrish, C.R., Tijssen, P., 2005. Parvoviridae. In: Fauquet, C.M., Mayo, M.A., Maniloff, J., Desselberger, U., Ball, L.A. (Eds.), Virus Taxonomy, VIIIth Report of the ICTV. Elsevier/Academic Press, London.

Yoon-Robarts, M., Blouin, A.G., Bleker, S., Kleinschmidt, J.A., Aggarwal, A.K., Escalante, C.R., Linden, R.M., 2004. Residues within the B′ motif are critical for DNA binding by the SF3 helicase Rep40 of adeno-associated virus type 2. J. Biol. Chem. 279 (48), 50472–50481.

Yu, D., Weller, S.K., 1998. Genetic analysis of the UL 15 gene locus for the putative terminase of herpes simplex virus type 1. Virology 243 (1), 32–44.

Yuan, W., Parrish, C.R., 2001. Canine parvovirus capsid assembly and differences in mammalian and insect cells. Virology 279 (2), 546–557.